https://doi.org/10.5194/egusphere-2024-927
Preprint. Discussion started: 14 May 2024

Seasonal and diurnal freeze-thaw dynamics of a rock glacier and their impacts on mixing and solute transport

Cyprien Louis[1], Landon J.S. Halloran[1,*], and Clément Roques[1,*]

[1]Centre for Hydrogeology and Geothermics (CHYN), University of Neuchâtel, rue Emile-Argand 11, 2000 Neuchâtel, Switzerland
[*]These authors contributed equally to this work.

Correspondence: Landon J.S. Halloran (landon.halloran@unine.ch) and Clément Roques (clement.roques@unine.ch)

Abstract. Rock glaciers play a vital role in the hydrological functioning of many alpine catchments. Here, we investigate seasonal and daily freeze-thaw cycles of the previously undocumented Canfinal rock glacier (RG) located in the Val d'Ursé catchment (Bernina Range, Switzerland) and the RG's influence on the dynamics of the hydrogeological system. We combine digital image correlation techniques, geochemical and isotopic analyses, time-series analysis, and hydrological monitoring to understand the functioning of the hydrological system. An acceleration of RG creep since 1990 has occurred, with the most active regions exhibiting horizontal velocities of ∼1 m/yr. Distinct geochemical signatures of springs influenced by RG discharge reflect contrasting and temporally-variable groundwater mixing ratios. A novel application of frequency-domain analysis to time-series of air temperature and spring electrical conductivity enables a quantitative understanding of the RG thaw and subsurface flow dynamics. A gradual decrease in time-lag between air temperature maximum and spring EC minimum, caused by dilution from RG ice melt, is observed over the snow-free period, implying progressively shorter residence times. Through our multi-method approach, we develop conceptual models for RG-influenced alpine hydrogeological systems on daily and seasonal time-scales.

1 Introduction

Rock glaciers (RGs) are one of the most common periglacial phenomena on Earth (Krainer et al., 2007). They can store significant volumes of water as ice and contribute significantly to catchment-scale fluxes during thaw (Harris et al., 2009). Rising temperatures and changes in precipitation are accelerating the thawing of RGs worldwide (Kääb et al., 2007; Marcer et al., 2021; Frei et al., 2018; Hanus et al., 2021; Manchado et al., 2024). Recent studies have quantified the role of groundwater in ensuring perennial streamflow under climate change scenarios in both glaciated (Somers et al., 2019) and non-glaciated (Halloran et al., 2023) alpine headwater catchments. Permafrost has also been shown to play a key role in delineating future spring locations (Evans et al., 2018). Rock glacier degradation is expected to have a significant impact on the alpine hydrological cycle, affecting the hydrology of downstream springs and streams (Jones et al., 2021). However, determining the long- and short-term dynamics of RG freeze-thaw cycles remains a major challenge (Pruessner et al., 2021). This knowledge gap stems from difficulties in collecting relevant data at such elevations, as well as a lack of understanding of the processes involved over pertinent time-scales. Difficulties lie in distinguishing between water fluxes from RGs and those from deeper groundwater flow

https://doi.org/10.5194/egusphere-2024-927
Preprint. Discussion started: 14 May 2024

paths, as well as in capturing their seasonal to daily variability (Krainer et al., 2015; Harrington et al., 2018) is challenging. Few studies that place RGs in their broader hydrogeological context have been conducted (e.g. Krainer et al., 2007; Del Siro et al., 2023; Munroe and Handwerger, 2023). As a result, seasonal variations in discharge sources such as groundwater, precipitation and snowmelt are often overlooked.

Environmental tracers provide unique information on the origin of waters, their residence times, and mixing during hydrological changes. Studies have used electrical conductivity (EC) as a tracer to complement water level data at alpine sites, taking advantage of its low cost and low probe maintenance requirements (Cano-Paoli et al., 2019). For example, EC can be used to separate hydrographs (Laudon and Slaymaker, 1997) or to analyse daily dilution/enrichment cycles of RG runoff on a seasonal or daily scale (Brighenti et al., 2021). Electrical conductivity (EC) is generally low during warm, high run-off periods, due to significant amounts of precipitation and melt-water, and high in autumn and winter when groundwater discharge is the primary driver of streamflow(Jones et al., 2019). Field campaigns for water sampling, on the other hand, face significant logistical challenges in alpine environments, limiting the ability to intervene at appropriate intervals to capture the variability of responses during high-frequency hydrological changes. Several authors have characterised the seasonal evolution of the composition of water discharge from RGs using isotopic analyses (in particular ^{18}O). These studies suggest that only a small fraction of the water released by RGs results from ice thaw (Krainer et al., 2007, 2015; Harrington et al., 2018).

The active layer has been shown to act as a thermal insulator between the surface and the frozen RG core (Humlum, 1997; Amschwand et al., 2023). It has a low thermal conductivity, which implies a different thermal regime between the RG and the outside. The ice is therefore partially insulated from external conditions, and thus thermally decoupled, making it more resilient to climate change than glaciers (Anderson et al., 2018; Jones et al., 2019, 2021). Analysis of displacement dynamics can aid in tracking the seasonal freeze-thaw dynamics of active RGs (Groh and Blöthe, 2019). The creep of active RGs is primarily caused by forces at the primary basal shear horizon (Krainer et al., 2015). The dynamics of RGs change over time and at different scales depending on the evolution of the RG thermal regime. It is mainly controlled by heat conduction driven by air temperature (T_{air}), but other processes such as advection of air or water through the RG matrix can also play a role (Haeberli et al., 2006; Pruessner et al., 2018). Several studies have found an increase in horizontal velocities as a result of rising temperatures in the Alps due to climate change (Kääb et al., 2007; Marcer et al., 2021). However, climate change affects not only T_{air}, but also the type and amount of precipitation (and hence, snow cover dynamics), the distribution of permafrost, and other parameters. In this context, several hypotheses have been proposed to explain variations in the horizontal displacement velocities of an active RG:

- In summer, high average and extreme T_{air} values favour the melting of RG ice, leading to destabilisation and acceleration (Marcer et al., 2021).
- Since adequate snow cover acts as a thermal insulator for the ground, a colder, snowier winter will tend to protect the active zone of the RG in early spring (DallAmico et al., 2008).

https://doi.org/10.5194/egusphere-2024-927
Preprint. Discussion started: 14 May 2024

- The early winter snow cover is important because it influences the thermal conditions underground by insulating the ground from the arrival of colder air. As a result, it is unfavourable for the preservation and formation of ice within the RG (Zhang, 2005).
- Intense precipitation in the form of rain has a destabilising effect due to the amount of water it can carry and the heat transfer it induces (Wirz et al., 2016).
- Influx of debris from rockfall events, which are, in turn, influenced by melting permafrost and weathering by rain, has an accelerating effect (Cusicanqui et al., 2021).

Here, we combine digital image correlation, hydrochemical analysis, and novel frequency-domain analysis of temperature and EC monitored at spring sites to resolve the seasonal and diurnal dynamics of an active RG. We determine multi-year trends in RG horizontal displacement and investigate how diurnal air temperature and spring electrical conductivity variations can provide information on RG-spring connectivity. This multi-faceted approach allows us to understand the complex hydrological and hydrogeological role of the Canfinal RG and can be applied to other alpine sites containing springs and permafrost features.

2 Study Area and instrumentation

The Canfinal rock glacier is located in the UNINE Poschiavino Observatory for Alpine Groundwater Research, and more precisely in the Val d'Ursé (Grisons, Switzerland) (Figure 1). It is a glacially formed, E-W oriented valley located in the Bernina Range (Western Rhaetian Alps, Switzerland) that feeds the main Val Poschiavo valley to the east. The geology consists of crystalline basement rocks and intruded granite of the Sella Nappe. The lower and middle parts of the valley are mostly Marinelli-Formation schist with Sella-Granodiorit (Lindsay, 2000). Musella-Granite and Sella-Granodiorit combine to form the southern ridges which feed the Canfinal RG. The Sella-Nappe is thrust over the Bernina-Nappe near the northern boundary of the Val d'Ursé and the nappe stack is part of a larger regional anticline. The hydrogeological system of the study site is made up of a fractured aquifer which is overlain by detrital sediments and coarse deposits. Several springs and groundwater seepage zones influenced by permafrost thaw have been identified across the watershed. They confirm the permafrost zones indicated by the Federal Office of Environment (Figure 1). Peak monthly precipitation occurs in October, November, and May, while February is the driest and coldest month (Lindsay, 2000). Several locations in the study area are intensely fractured, which may allow for efficient groundwater recharge. Infiltration is expected to be greatest on gentle slopes with exposed permeable material such as debris and talus deposits or fractured bedrock. On steep slopes with low permeability material, such as sub-glacial moraines or intact bedrock, the infiltration is low.

This alpine site (Figure 1) benefits from a borehole of 200.3 m depth, which is equipped with two pore water pressure sensors (KB4). Additionally, the EC and temperature of several springs (Figure 1) are monitored.

https://doi.org/10.5194/egusphere-2024-927
Preprint. Discussion started: 14 May 2024

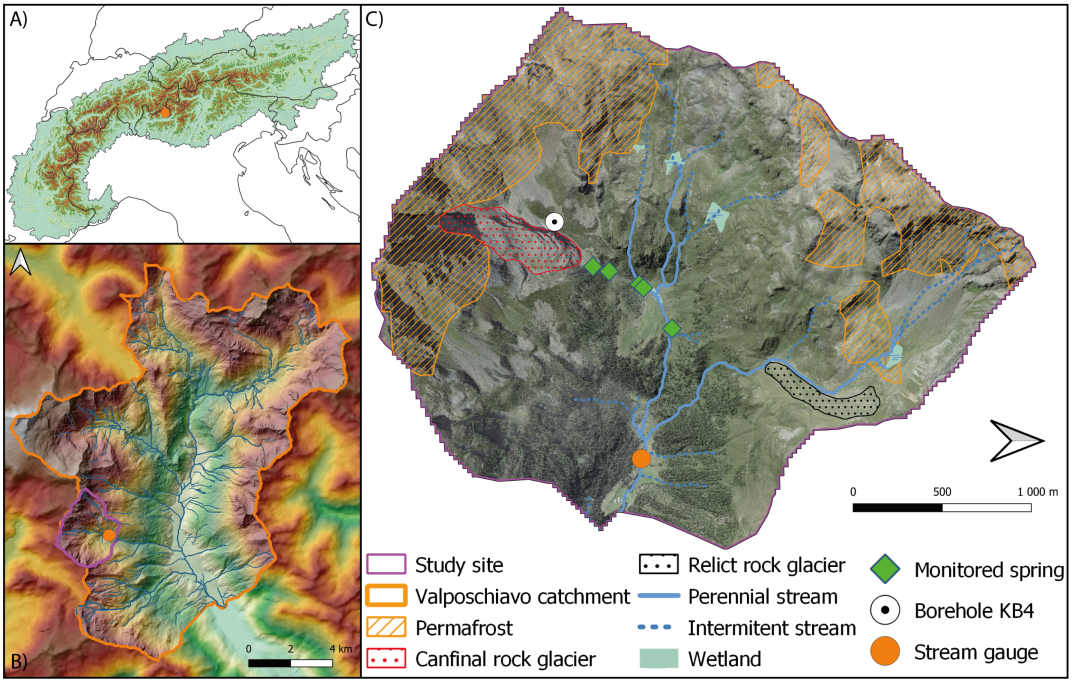

Figure 1. Location of study site *A)* in relation to the Alps and *B)* within the Valposchiavo catchment. *C)* This headwater catchment is characterized by the presence of permafrost (FOEN Switzerland, 2005), two major RGs, and wetlands. Selected environmental monitoring points are also indicated.

A former glacier front, associated with the Cavaglia local glacial stage (Egesen I), reached an elevation of 2160 m a.s.l. with an equilibrium line at ∼2450 m where the Canfinal RG now stands (Burga, 1987). Rockfalls from the cliffs filled the moraine valley of this retreated or partially retreated glacier, and favourable permafrost conditions led to the formation of the Canfinal RG. There are also signs of lateral moraines located beneath the RG. The RG has a length of ∼820 m, a maximum width of ∼250 m, and a surface area of ∼0.2 km^2. Its front is located at an elevation of ∼2220 m and faces northeast. Its rooting zone begins at an elevation of ∼2500 m, at the base of a ridge. This cliff links the Piz Canfinal (2812 m) to the Corno Compascio (2808 m) and contains several weak zones feeding debris to the RG. Longitudinal ridges in the upper part are a sign of sharp contrasts in horizontal displacement between the center and the edge of the RG. The presence of longitudinal ridges in the lower section indicates a lower flow (Figure 2). The RG's lower foot is more vegetated and appears to be separated from the rest. Although it will be considered as a whole in the context of this study, the entire structure is most likely the result of several generations of RGs, some of which are now inactive or relic (Figure 2).

https://doi.org/10.5194/egusphere-2024-927
Preprint. Discussion started: 14 May 2024

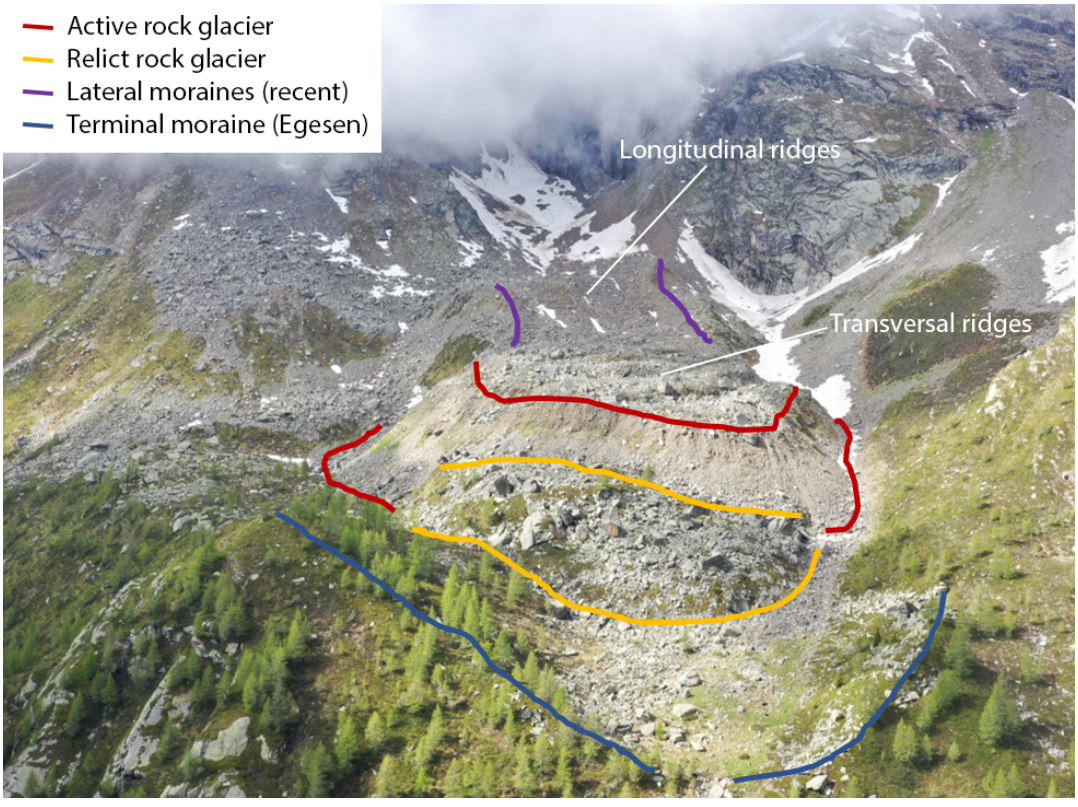

Figure 2. Basic geomorphological description of the Canfinal RG and its surroundings. Additional information on Quaternary geological and geomorphological features in the Val d'Ursé can be found in Figure S1 (SI).

Numerous perennial and intermittent springs immediately downslope from the RG indicate a shallow and dynamic water table that reaches its maximum near the end of the snowmelt season. The spring at the foot of the Canfinal RG is located at ∼2210 m in a relatively flat, humid meadow. During periods of high runoff and snowmelt, another spring is active at the mid-slope of the talus, while the majority of the springs at the foot of the talus slope are perennial and feed the Val d'Ursé.

3 Methodology

3.1 Digital image correlation

Digital image correlation is a powerful method to calculate rock glacier displacement fields (e.g., Amschwand et al., 2021) based on snow-free remote sensing imagery. We analysed the historical and present rheological dynamics of the Canfinal RG using 13 largely snow-free SWISSIMAGE ortho-rectified photos (swisstopo) from between 1956 and 2019 and data from an unmanned aereal vehicle (UAV) survey from October 2022. The ortho-photos have a pixel resolution of 0.5 m for the oldest

https://doi.org/10.5194/egusphere-2024-927
Preprint. Discussion started: 14 May 2024

(1956–2003), 0.25 m for the 4 images taken between 2006 and 2015 and 0.1 m for 2019. Using the *PIX4DMapper* software, the photos from our UAV survey were converted into an ortho-photo with a resolution of 2.7 cm.

We used an open-source fast Fourier transform (FFT)-based digital image correlation open source package (Bickel et al., 2018). Before co-registration, the software pre-processes images via a Wallis filter in order to reduce noise and improve contrast (Baltsavias, 1991). Displacement is calculated across image pairs. The co-registration algorithm works by selecting a reference block of pixels with sufficient optical contrast in the first (oldest) ortho-image. In the second ortho-image, the algorithm searches for the same block in a test area. If the block is successfully detected, a local horizontal displacement vector between the two images is calculated by the difference via the coordinates of the centroid. In our application, only vectors with a RMSE under a defined threshold, depending on the resolution of the orthophotos, are kept. This filtering enables exclusion of spurious data from steep slopes and in cliff-adjacent areas that are frequently covered by loose debris or snow.

3.2 Hydrochemistry and tracers

Five sampling campaigns of 37 springs and stream locations were conducted between July 2022 and June 2023 (Figure 3).

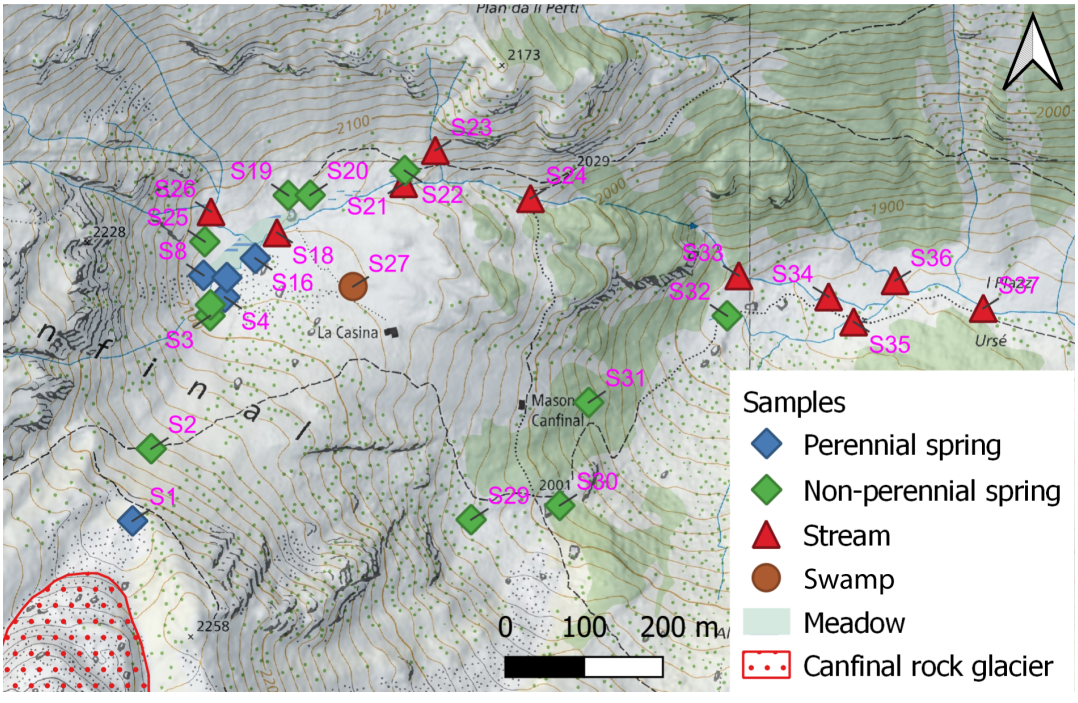

Figure 3. The various springs and streams from which samples were collected during five campaigns between July 2022 and June 2023 for hydrochemical and isotopic analysis. The Val d'Ursé stream gauge is at the same location as the sampling point S37. Springs S1 - S4 and S23 were also equipped with a temperature/EC probes.

Principal component analysis (PCA) was performed to statistically analyze the composition of the water samples and to differente water sources. The considered variables were stable isotopes (δ^{18}O and δ^{2}H, ‰ with respect to VSMOV), EC, and

https://doi.org/10.5194/egusphere-2024-927
Preprint. Discussion started: 14 May 2024

concentration of the following ions: Cl^-, NO_3^-, SO_4^{2-}, Na^+, K^+, Ca^{2+} and Mg^{2+}. We used the *python* package *scikit-learn* (Pedregosa et al., 2011) and the *R* packages *FactoMiner* (Lê et al., 2008) and *factoextra* (Kassambara and Mundt, 2020) with variable standardization (scaling and centring) for PCA of all the data, and also for the dataset corresponding to each field mission. This analysis was completed by correlation matrices made with the *R corrplot* package (Wei and Simko, 2021). Only significant correlations were considered ($\rho < 0.05$). The seasonal evolution of the isotopic data was compared to a local meteoric water line (LMWL) corresponding to an average of four northern regions of Italy bordering the catchment (Longinelli and Selmo, 2003; Longinelli et al., 2006):

$$\delta^2 H(‰) = 7.6 \times \delta^{18} O + 9.4 \quad (1)$$

3.3 Frequency-domain analyses of spring time-series

Frequency-domain analyses of hydrological time-series can offer novel insights into hydrological processes (e.g., Acworth et al., 2017; Rau et al., 2017; Houben et al., 2022). Here, we perform this analysis on data from springs that are at least partially fed by melt from the RG. Temperature and EC from four springs situated at the foot of the Canfinal RG (S1), in the middle of the talus (S2) and at the talus/meadow interface (S3 and S4) (Figure 3) were monitored. The recording interval was 10 minutes (July–October 2022) and 30 minutes thereafter. Specific conductance (EC at 25°C) was calibrated with measurements taken by a portable probe (Cond-3310). A rolling-window FFT was used to isolate the dominant diurnal, i.e. 1 cycle-per-day (cpd) signal of the EC and air temperature (T_{air}) time-series. Days that were heavily influenced by dilution due to heavy rainfall events, as well as periods when the springs were dry, were excluded. A 3-day window length with a 1-day step was selected to balance temporal resolution and noise reduction, and to avoid eliminating excessive amounts of data adjacent to excluded time-series data points.

Diurnal (i.e., frequency f =1 cpd) signals with non-stationary amplitude and phase dominate the air temperature (T_{air}) and S1 and S4 specific conductance (EC_{S1} and EC_{S4}) time-series. Amplitude (A) is a measure of the intensity of the diurnal variation, while phase (ϕ) or, similarly, time-lag is a measure of the time of day that minimal and maxima occur. Here, to aid interpretation, we present the data as a shifted time-lag (Δt):

$$\Delta t = \frac{24\text{h}}{2\pi}\left(\phi + \frac{\pi}{2}\right) = \frac{24\text{h}}{2\pi}\phi + 6\text{h} \quad (2)$$

where ϕ is implicitly defined, noting the sign convention here, in the sinusoid:

$$f(t) = A\sin(2\pi t/(1\text{ day}) - \phi) \quad (3)$$

The time-lag is then limited to the range of $[0\text{h}, 24\text{h})$ by shifting values outside this range by multiples of 24 h. Thus, a sinusoid with a phase $\phi = 0$ corresponds to a time-lag of 06:00 UTC+0, i.e. the time of day at which the function is at its maximum. In a hypothetical case where maximum temperature coincides with minimum EC, the signals would be completely out of phase and thus the time-lag between them would be ± 12 hours.

https://doi.org/10.5194/egusphere-2024-927
Preprint. Discussion started: 14 May 2024

4 Results

4.1 Inter-annual dynamics derived from photogrammetry

The RG horizontal velocity field (Figure 4) shows a high degree of spatial and temporal variability. For the most recent period (2019–2022), the horizontal velocity is highest in the centre of the upper part of the RG. Here the average horizontal velocity
155 can slightly exceed 1 m year $^{-1}$. A decreased velocity is observed in the lower, central part where horizontal ridges are visible. At the edges of the RG and in the frontal zone, creep is negligible.

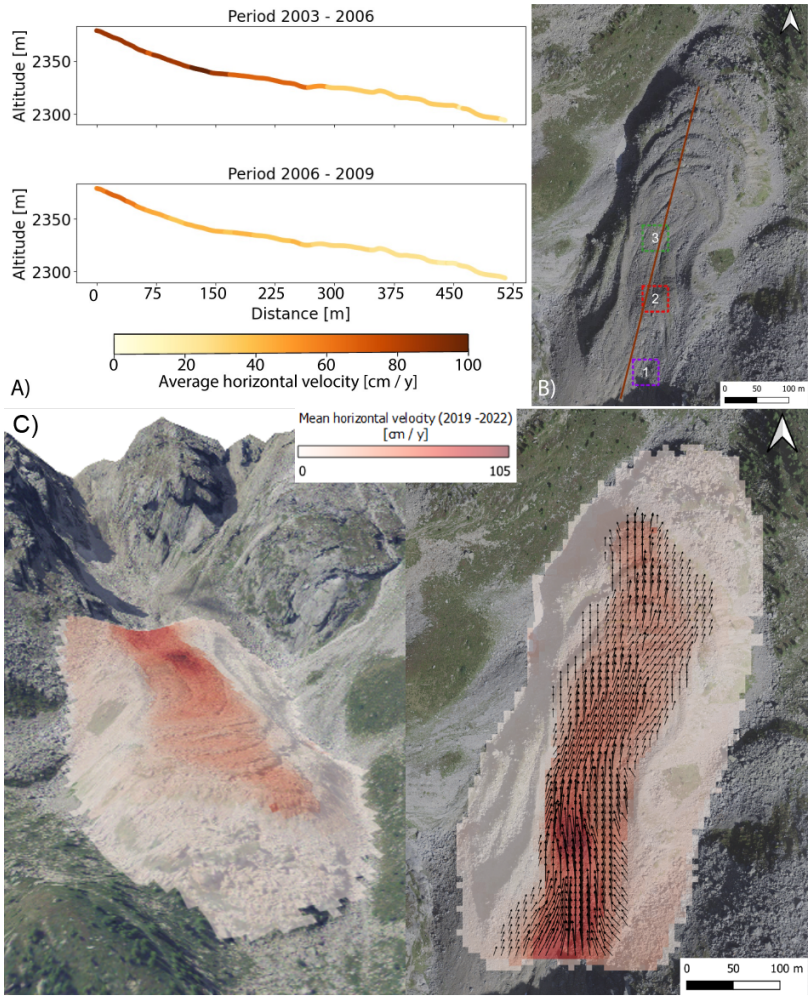

Figure 4. *A)* Average horizontal velocity along the topography between the contrasting periods 2003–2006 (high activity) and 2006–2009 (low activity). *B)* The three zones in the upper part of the Canfinal RG for which recent changes in average horizontal velocity have been compared (see text). *C)* 3-D and top-down views of average horizontal velocity of the Canfinal RG for the period 2019–2022. Vectors represents the horizontal displacement direction and intensity.

https://doi.org/10.5194/egusphere-2024-927
Preprint. Discussion started: 14 May 2024

The differences in average horizontal velocity along the topographic profile of the RG confirm that velocities are highest in the upper part. Average horizontal velocities for three 40 m × 40 m zones in the upper part were compared with six climate indicators for the period 1990 to 2022:

- Summer temperature anomaly: Mean daily T_{air} anomaly for the summer period (June–August) compared to the mean summer T_{air} measured since 1940 (data: ERA5 (Hersbach et al., 2023)).
- 5% of hottest days: Number of summer days (JJA) per year when the mean T_{air} is higher than 95% of the daily summer mean T_{air} measured since 1940 (data: ERA5).
- Winter days: Number of days per year when the average T_{air}, as defined by Meteosuisse, is below 0°C (data: ERA5).
- End of 10 cm snow cover: date when the snow cover falls below 10 cm (data: ERA5).
- December snow depth anomaly: anomaly of the mean snow depth at the beginning of the winter season, i.e. in December (data: ERA5).
- 5% of wettest days: Number of days per year on which the cumulative precipitation is greater than 95% of the daily cumulative precipitation measured since 1990 (data: Meteoswiss Station "Poschiavo/Robbia").

The results show a general acceleration of the average horizontal velocity since the 1990s (Figure 5), especially for zones 2 and 3 (Figure 4b). The average horizontal velocity in zone 2 was 39±6 cm year^{-1} between 1992 and 2003, while its maximum was measured between 2019 and 2022 with 71±5 cm year^{-1}. In zone 3, the average velocity was 32±6 and 52±5 cm year^{-1} for the same two periods, but peaked at 72±9 cm year^{-1} between 2003 and 2006. The variations are less significant for zone 1, which nevertheless experienced a slowdown in the period 2010 - 2012 (37±12 cm year^{-1}). This stabilisation is also visible in zone 2.

Only the climate indicators for the summer T_{air} anomaly and days with extreme temperatures show a similar overall trend that can be attributed to climate change. All three zones experienced a strong acceleration between 2003 and 2006, with 2003 being characterised by a very warm summer T_{air} anomaly (>2°C) and a high number of days (24) with extreme temperatures. These values correspond to the European heat wave of 2003. It should also be noted that 2014 had a strong winter with a significant snow depth anomaly that lasted until May. There were also less intense precipitation events, and the summer was characterised by a negative T_{air} anomaly and few extremely warm days. In the following years, from 2015 to 2019, there was a slowdown in zones 1 and 3 and a stabilisation in zone 2. Otherwise, there are no globally similar trends between the acceleration and stabilisation phases of the three zones and the winter indicators or with intense precipitation events.

https://doi.org/10.5194/egusphere-2024-927
Preprint. Discussion started: 14 May 2024

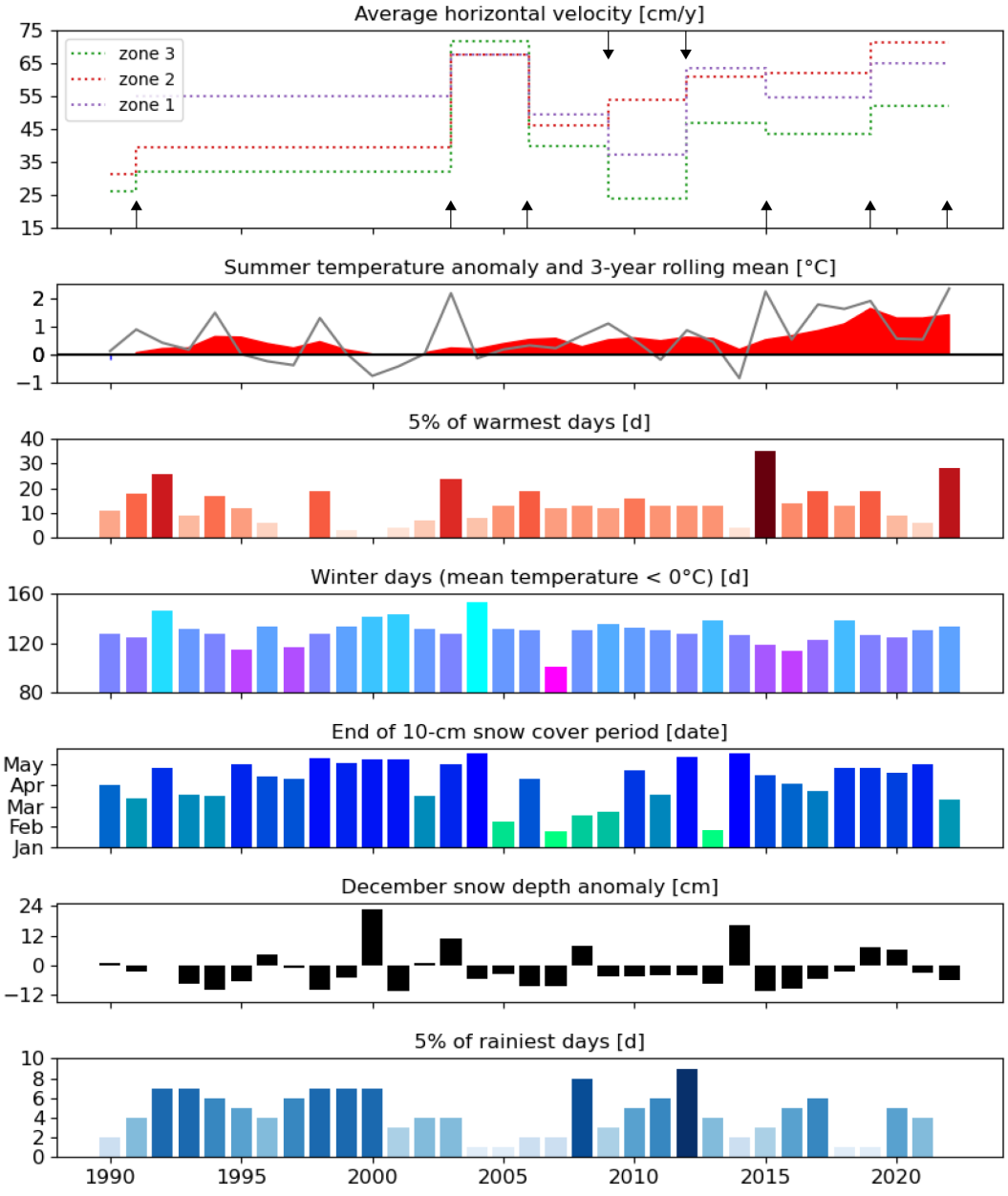

Figure 5. Recent evolution (1990–2022) of the Canfinal RG zonal dynamics in comparison with various summer and winter climatic indices. The 7 orthoimages available since 1990 and the drone acquisition in 2022 are indicated by an arrow. For zone definitions, see Figure 4b.

https://doi.org/10.5194/egusphere-2024-927
Preprint. Discussion started: 14 May 2024

4.2 Seasonal evolution of water sources at the springs

All ionic concentrations are low, which is expected for this alpine environment dominated by crystalline basement rock. Springs situated at the front of the Canfinal RG (S1) and in the talus (S2) (Figure 3) have a higher K^+ concentration. S1 and S2 are also more enriched in heavy stable isotopes and have higher NO_3^- and Na^+ concentrations than the springs situated at the talus/meadow interface (S3, S4, S5, S13 and S16). The latter are more mineralised and form a distinct group, with higher Ca^{2+} and Mg^{2+} concentrations and EC, elements again almost completely correlated (r-values: 0.97–0.99). They also contain fewer heavy isotopes (r-value of -0.69 between the EC and $\delta^{18}O$ and -0.6 between the EC and δ^2H). NO_3^- and K^+ are again positively correlated (r = 0.72). S1 has the highest concentration of NO_3^- (1.85 mg L^{-1} or 0.03 meq L^{-1}) and their proportion decreases along the talus/meadow complex as a function of distance from the RG. The perennial spring S4 at the talus/meadow interface has a NO_3^- concentration of 1.35 mg L^{-1} (0.022 meq L^{-1}), while all other springs located in the meadow area, but not aligned with the RG and the talus, have NO_3^- concentrations ranging between 0.004 to 0.014 meq L^{-1}.

High Cl^- concentration and an isotopic enrichment distinguish samples S27 and S29. S29 is a non-perennial spring located away from the others, at the foot of an outcrop belonging to the Marinelli formation, and S27 is located in a wetland. There is a positive correlation between Cl^- concentrations and δ^2H and $\delta^{18}O$ enrichment (r = 0.58 and 0.61, respectively). Groundwater coming from the debris cones situated at the foot of the northern flank of the study area (springs S20, S22, S23, and S26) is less mineralised. The water of the main stream is distinguished from the springs by its higher Na^+ concentration. PCA restricted data from an Oct 2022 sampling campaign shows clear differences in the different springs (Table S1 and Figure S2 in supplementary information, SI) as his sampling campaign occurred after a prolonged dry period during a time of the year when groundwater's contribution to streams is expected to be significant in alpine environments (Somers and McKenzie, 2020; Hayashi, 2020).

Isotopic data from springs and streams show an enrichment of heavy stable isotopes ($\delta^{18}O$ and δ^2H) in summer and autumn 2022 as a function of the number of days elapsed after the end of snowmelt (Figure 6A). The values for June 2023 correspond to the melting of the snowpack and are significantly lower. The first two axes of the PCA explain 66.7% of the total variation in the data set corresponding to the five sampling campaigns (Figure 6B). The bi-plot of samples and variables verifies the isotopic enrichment and shows an increase in Na^+ and K^+ concentrations during the summer. The gradient of stable isotopes and Na^+ along PC2 distinguishes the different sampling campaigns. The data from June 2023 are more uniform than for other periods when the snowpack was no longer melting. There is a positive correlation with an r value of 0.76 between NO_3^- and K^+ (Figure 6C). Other significant correlations shown in the matrix include the positive ones between Na^+ and EC (r = 0.45), Ca^{2+} (r = 0.48) and Mg^{2+} (r = 0.49). Furthermore, there is a strong positive correlation between EC, Ca^{2+}, Mg^{2+} and SO_4^{2-} (r values between 0.95 and 0.99).

https://doi.org/10.5194/egusphere-2024-927
Preprint. Discussion started: 14 May 2024

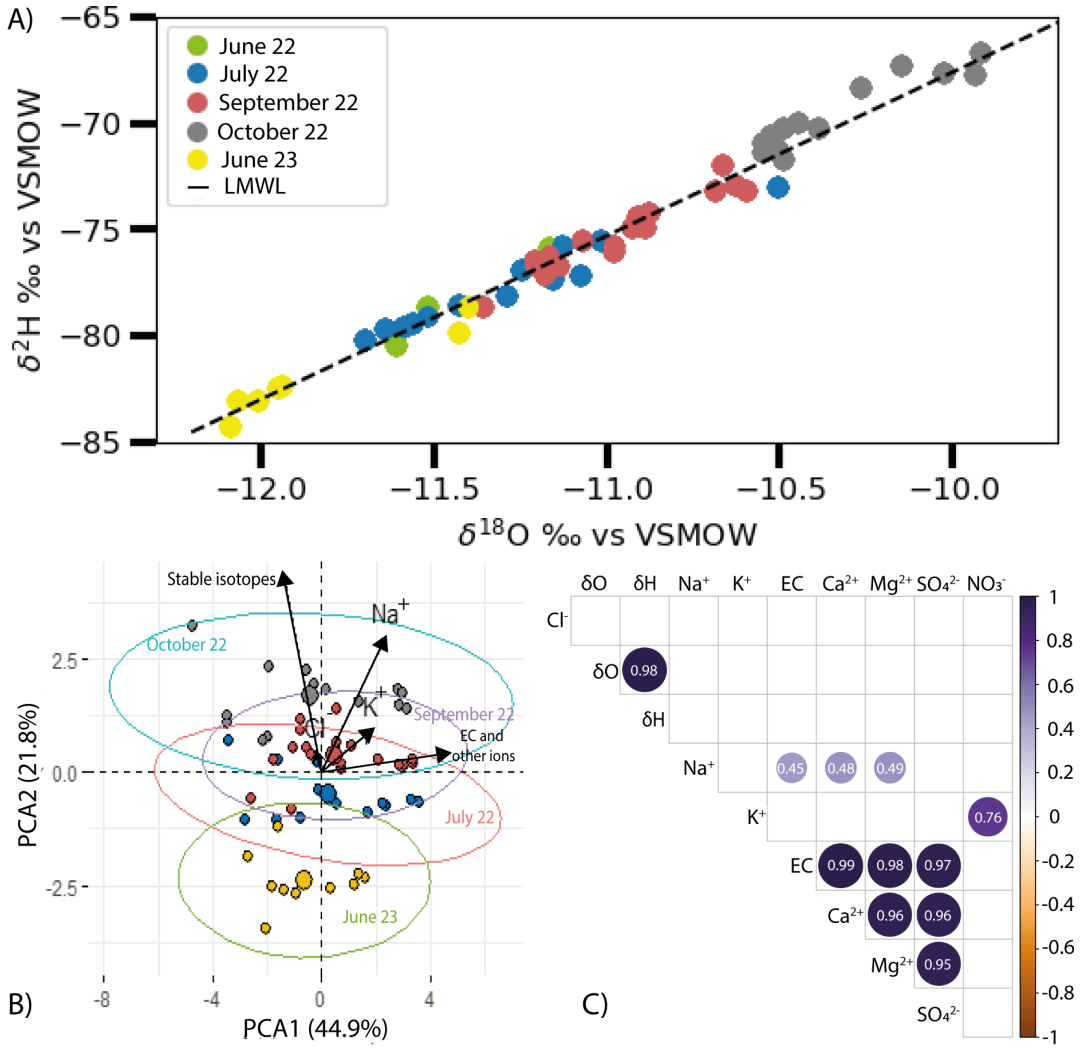

Figure 6. A) Isotopic values of all samples taken between July 2022 and June 2023 in comparison with the local meteoric water line (LMWL)(Longinelli and Selmo, 2003; Longinelli et al., 2006). B) Principal component analysis (PCA) bi-plot with ellipses grouping the different sampling campaigns. C) Correlation matrix containing only the significant correlations between variables ($\rho < 0.05$). The colour intensity and size of the circles are determined by the strength of the correlation (purple = positive correlation, gold = negative correlation). The number represents the correlation coefficient (r) for each correlation. A similar analysis of only the Oct 2022 samples can be found in the SI document (Figure S2).

4.3 Frequency-domain analyses of dilution linked to RG diurnal thaw cycles

EC time-series measurements from the springs (Figure 7) showed varying responses at the foot of the RG (S1), in the mid-slope of the talus (S2), and at the talus/meadow interface (S3 and S4). The following observations can be made:

https://doi.org/10.5194/egusphere-2024-927
Preprint. Discussion started: 14 May 2024

- S1: Rainfall events have a strong dilution effect at the end of summer and in autumn, and the EC increases systematically between two events, with an observed increase throughout the summer. In the autumn of 2022, there were some extremely dry periods and the spring dried up several times between September and October and is also dry during most of the snow cover period. Nonetheless, it should be noted that beneath the talus slope immediately down-gradient of S1, flowing water was observed throughout the snow-free period. In 2023, the spring was reactivated at the beginning of May with the melting of the snow cover, resulting in a lower EC (about 40 μS cm^{-1}) than before the winter.

- S2 is active in spring due to snowmelt and was also active during a field campaign in June 2022 (before the probes were installed). The data show two activations of S2 due to heavy rainfall events in summer and autumn.

- Springs S3 and S4, located at the talus/meadow interface and feeding perennial streams, have the very similar EC values when both are active. S4 is perennial whereas S3, located ~10 m away and ~2 m higher, often dries up in late summer and autumn. The EC of S4 increases at the end of the summer season and remains stable during the winter. Dilution by snowmelt then began in mid-March.

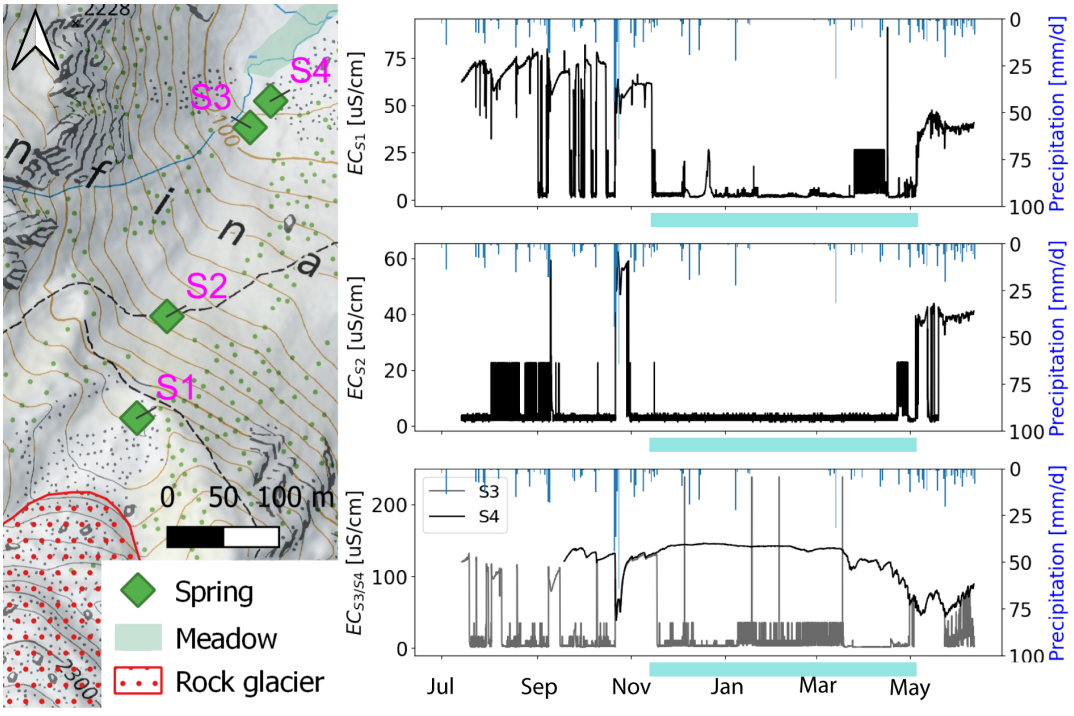

Figure 7. Electrical conductivity measured between July 2002 and June 2023 of the springs at the foot of the Canfinal RG (S1), mid-slope of the talus (S2) and at the talus/meadow interface (S3 and S4). Daily precipitation and duration of the snow cover period (turquoise bar) are also indicated. EC values near 0 μs/cm indicate non-flowing (dry) springs.

https://doi.org/10.5194/egusphere-2024-927
Preprint. Discussion started: 14 May 2024

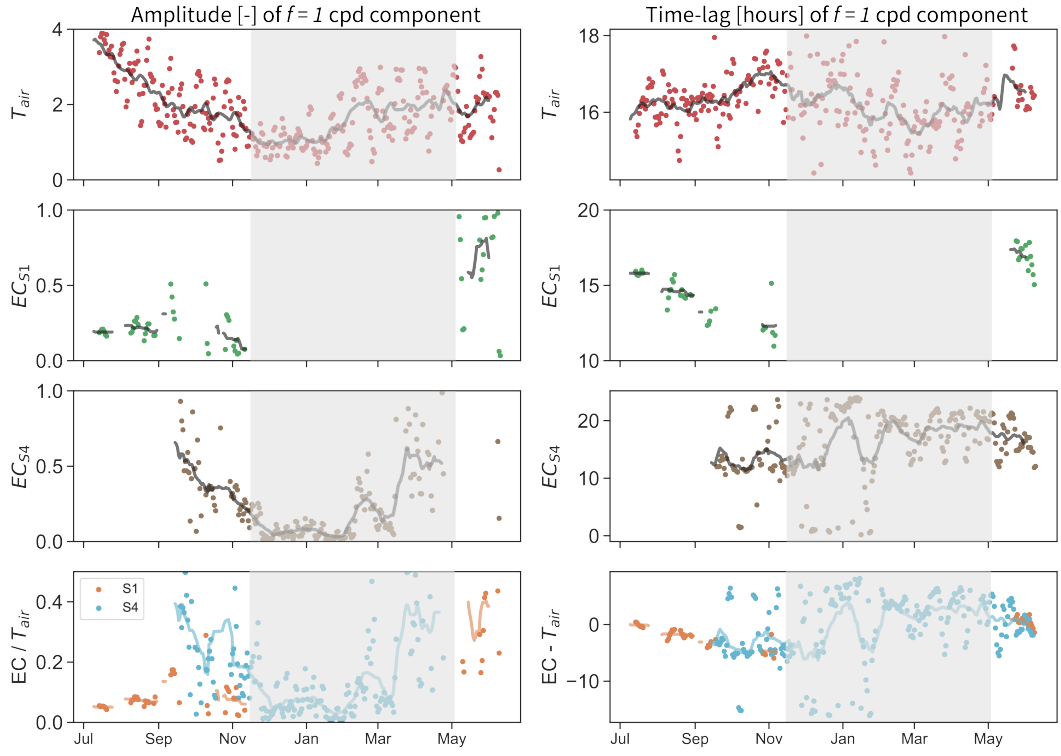

Figure 8. Amplitude (left) and time-lag (right) of 1 cpd components of the filtered EC time-series from springs S1 (foot of the Canfinal RG) and S4 (talus/meadow interface) and air temperature between July 2022 and June 2023. The relative amplitude ratio and time-lag (analogous to phase) difference between the springs and air temperature signals are also illustrated. Rolling means with a 21-day window length are also shown in order to help discern seasonal trends. Here, amplitudes can be considered unitless and phase has been converted to a time-lag (i.e., from radians to hours UTC+0) to facilitate interpretation (Section 3.3). The period of snow cover (mid-Nov. 2022 to early May 2023) is indicated by the shaded section.

The amplitude and phase of the 1 cpd components of T_{air}, EC_{S1} and EC_{S4} were calculated using a 3-day rolling window stepped in increments of 1 day (Figure 8). Frequency-domain analysis of these time series in reveals significant amplitude variations and a phase lag between the T_{air} and EC signals measured at these springs. S2 and S3 (Figure 7) are not analysed here due to their lack of extended active periods. The 1 cpd amplitudes vary significantly for all datasets, indicating seasonal differences in the intensities of daily cycles. T_{air} varies more diurnally during summer than winter, as indicated by its amplitude trend. The amplitudes of the spring EC diurnal variations also exhibit seasonal trends which, for the snow-free period, can be interpreted as measures of the intensity of dilution from RG melt. S1, at the foot of the RG, shows a much higher variation in period immediately after snowmelt than it does in the summer and autumn period; however, it is possible that this may be due to snow accumulation and subsequent melt in the RG itself. Nonetheless, the relatively constant, low amplitude values of S1 in the late summer and autumn, as compared to the down-gradient S4 spring, suggest significant influence from a deeper groundwater component unaffected with a stable temperature. The ratio of the EC 1 cpd amplitudes to those of T_{air} normalises

https://doi.org/10.5194/egusphere-2024-927
Preprint. Discussion started: 14 May 2024

the EC amplitudes by the main driver of daily melt rate variations. S4 shows significant variations before the onset of snow, indicating a potentially significant contribution from RG meltwater.

The phase, or time-lag, information enables an objective measurement of the timing of diurnal dilution processes. The phase of the 1 cpd component of T_{air} is, as expected, relatively stable throughout the year. S1 exhibits decreasing trend before the onset of snowfall indicating that the times of maximum and minimum daily EC occur progressively earlier over this period. The phase of S4 shows a less discernible trend over the same period, with the EC maximum appearing to be relatively stable, although at the beginning of the snowfree period in 2023, the time-lag is greater, as is also observed in S1. The phase shift, or time-lag, between EC and T_{air} confirms these observations, although little difference is observed because of the relatively stable T_{air} phase. Nonetheless, we can observe that the EC daily maxima generally precede the T_{air} maxima and thus the EC daily minima lag T_{air} by <12 hours.

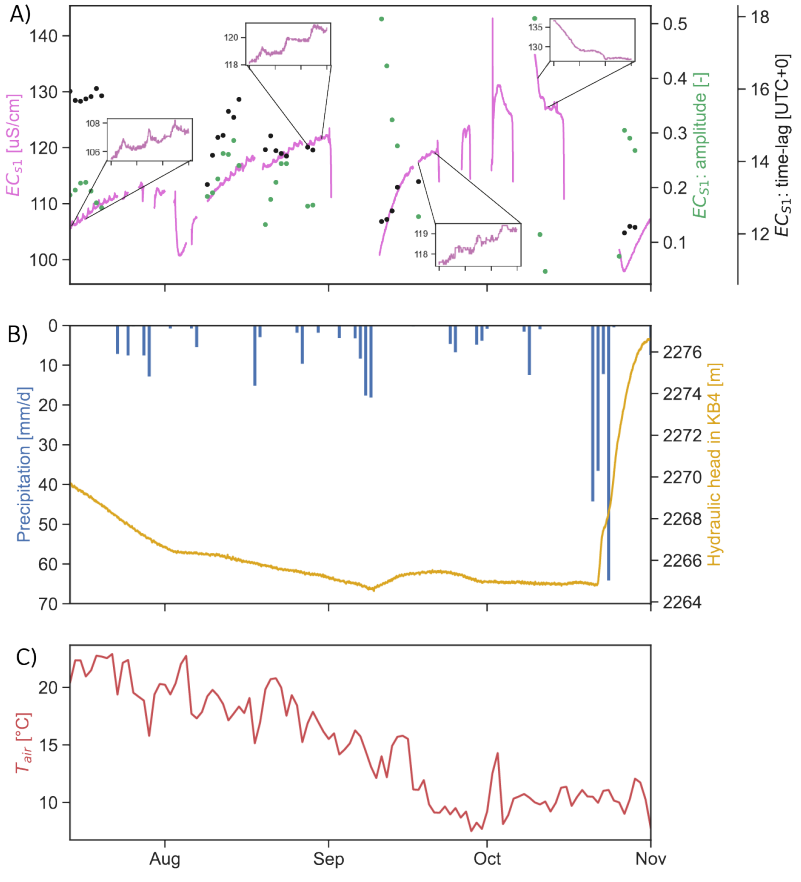

Figure 9. A) Filtered electrical conductivity of spring S1 as well as the amplitude and time-lag of the 1 cpd frequency component (see Figure 8) for the period 14.07.2022–01.11.2022. Periods with no data represent days with precipitation or spring flow cessation. Detail of selected 3-day windows is also shown to illustrate the variations in daily variations. B) Fractured aquifer hydraulic head (KB4, see Figure 1) and daily rainfall (mm) over the same time period. C) 7-day average air temperature (° C, ERA5).

https://doi.org/10.5194/egusphere-2024-927
Preprint. Discussion started: 14 May 2024

The longer-term, non-diurnal trends in EC and hydraulic head also give insight into the local hydrological process. During the summer and autumn snow-free period, the EC of spring S1 rises gradually (Figure 9a). The hydraulic head in borehole KB4, adjacent to the RG (Figure 1), responds non-linearly to precipitation events (Figure 9b). The minimum hydraulic head (early September) recorded at KB4 corresponds to a period at which spring S1 was dry. The general cooling temperature trend over this period coincides with a decrease in amplitude and a negative shift in time-lag of EC_{S1}. Lower temperatures are expected to result in a lower rate of RG thaw.

5 Discussion

5.1 Creep is accelerating as a result of rising temperatures

Horizontal velocity patterns of Canfinal RG are consistent with the presence of longitudinal ridges in the upper part of the RG, indicating strong velocity contrasts between the centre of the RG (1 m year^{-1}) and the edges. The horizontal ridges in the lower part confirm the stabilisation of the displacement. We can conclude that the upper part is active, while the lower part consists of older features that are now inactive or relicts. Since 1990, the zones delineated in the upper active part, especially zones 2 and 3 (Figure 4b), which are further away from the cliffs, have accelerated. This is the steepest part of the RG and also the zone for which most conceptual models indicate the largest proportion of ice (Jones et al., 2019; Schaffer et al., 2019), making this higher velocity a good indicator of the presence of a large amount of supersaturated debris/ice mix under steady-state creep. This demonstrates that, in addition to slope, the volume and temperature of the ice, which affect its rheology, as well as the increase in liquid water content caused by thawing, have significant impact on the dynamics of RGs (Duval et al., 1983; Kääb et al., 2007; Marcer et al., 2021). Nonetheless, most of the horizontal RG displacement is observed in the shear horizon. It is located at the base of the RGs and the effect of T_{air} is therefore delayed and limited (Kääb et al., 2007; Cicoira et al., 2021). Temperature variations within the shear horizon are thought to alter its mechanical properties over longer time scales, particularly those near the melting point. The presence of pressurised water within this unit suggests that the unfrozen water content has a strong influence on its dynamics (Ikeda et al., 2008; Buchli et al., 2018; Cicoira et al., 2021). In addition, melting ice allows more liquid water to enter the shear horizon, with the associated destabilising effect and heat conduction (Wirz et al., 2016).

Although the determined horizontal velocities are multi-year averages, the trends appear correlated to the summer T_{air} anomaly and the number of days with extreme T_{air} (Figure 5), both of which are increasing in the Alps due to global warming. This observation is consistent with the results of several studies in the Alps indicating acceleration of RGs as a result of rising temperatures (Kääb et al., 2007; Marcer et al., 2021). We note, however, that recent deceleration has been observed at four RGs, at similar elevations to the Canfinal RG, but situated immediately down-gradient of glaciers, in the Swiss National Park (Manchado et al., 2024). 2014 saw a colder summer and it appears that this may have had a stabilising effect in the following years. In fact, this event was also highlighted by Cusicanqui et al. (2021) for a RG in the French Alps. A strong acceleration after the European heat wave of 2003 was also observed for many other RGs in the Swiss Alps and western Austria (Krainer and He, 2006; Delaloye et al., 2010). These similarities suggest that active RGs in the same geographical area tend to be

https://doi.org/10.5194/egusphere-2024-927
Preprint. Discussion started: 14 May 2024

affected in the same way by summer temperature extremes. Although it has been shown that precipitation can cause short-term acceleration of RGs (Wirz et al., 2016), our results lack the temporal resolution to confirm this. There is no visible relationship between the average velocity changes and the winter indicators. One explanation could be that the long-term activity of the RG is mainly influenced by T_{air} and/or that the other parameters have no significant effect in comparison. It is also possible that confirmation of stabilising or accelerating effects of the various indicators (Figure 5) requires data with a higher temporal resolution.

5.2 Seasonal variations in spring end-members reveal freeze/thaw and transport dynamics

Enrichment in heavy stable isotopes is observed for all springs and streams during the summer, while the hydraulic head of the fractured aquifer and the water level of the Val d'Ursé decrease during the same period. This indicates that the contribution of groundwater increases after the end of snowmelt and maintains the baseflow of the catchment. This enrichment can also be explained by a higher contribution of enriched meteoric water formed at higher temperatures than winter snow, increased evaporation from open surfaces in summer and/or the release of meltwater from permafrost that has undergone several freeze/thaw cycles and induces recharge at higher altitudes (Williams et al., 2006; Moran et al., 2007; Beria et al., 2018; Brighenti et al., 2021). The rise in the Val d'Ursé EC over the same period confirms that the water of the fractured aquifer is more mineralised and compensates for the significant and visible dilution effect of rainfall events and the expected dilution effect of permafrost, Canfinal RG ice and frozen ground freeze/thaw cycles. The Val d'Ursé reaches an EC peak in summer, a phenomenon that is particularly visible in 2020. According to Colombo et al. (2019), these types of maxima may correspond to the maximum thaw rate of permafrost or frozen ground. The values then decrease due to the decrease in T_{air} and the amount of solar radiation, which helps to cool the permafrost and the RG active layer. An isolated contribution from the Canfinal RG cannot be detected in the signals from borehole KB4 and EC and the water level of the Val d'Ursé, and thus at the headwater catchment scale. This is in agreement other RG studies that have determined contribution to total discharge by active RGs to be $\lesssim$5% (Krainer et al., 2015; Harrington et al., 2018).

The PCA performed on the October 2022 samples (Figure S2) shows that the springs closest to the Canfinal RG (S1 and S2) have a distinct geochemical signature. They are characterised by a higher concentration of K^+ and Na^{2+} and the greater enrichment of heavy stable isotopes. The fact that rock weathering is thought to be the main driver for the presence of certain trace elements in RG runoff helps to explain the high concentration of K^+ and Na^{2+} (Colombo et al., 2018). In fact, the rocks that make up the debris of the RG and the surrounding cliffs are orthogneiss (Sella granodiorite) with muscovite and feldspars, and a granite intrusion (Musella granite) rich in biotite and feldspars. The concentrations of NO_3^- are higher between the RG and the talus-meadow interface than in other springs in the Val d'Ursé. Studies have highlighted this peculiarity in the discharge of RGs and blockfields (Williams et al., 2007; Colombo et al., 2019). Some suggest that bacterial activity in RGs is the cause of this enrichment. These extreme environments, with snow cover in winter, low light levels and stable, cold soil temperatures around 0°C, are carbon limited and can support nitrifying bacterial communities. According to Del Siro et al. (2023), it could also be atmospheric pollutants released by melting ice. These results lead us to conclude that the presence of the Canfinal RG and the lithology of its constituent rocks influence the hydrochemistry of the springs fed by its discharge. The

https://doi.org/10.5194/egusphere-2024-927
Preprint. Discussion started: 14 May 2024

higher isotopic values of the discharge from the RG could be explained by easier infiltration of water from summer rainfall events into it (Krainer et al., 2007), or by an altitudinal gradient, as proposed by Moran et al. (2007).

5.3 RG diurnal discharge dynamics is revealed through frequency-domain analysis

Analysis of the EC diurnal signals of the spring at the foot of the Canfinal RG (S1) shows the existence of a daily cycle of dilution/enrichment. Dry periods are characterised by an increase in the EC of the discharge over several days, influenced each day by a dilution that starts in the afternoon. Although the discharge rate could not be measured, available studies indicate a maximum discharge rate in the afternoon, corresponding to the meltwater supply of the RG (Krainer and Mostler, 2002). As these waters are expected to be low in total dissolved solids, the diurnal RG discharge peak is expected to correspond to the S1 EC minimum due to its dilution effect. This occurs with a time-lag (or phase lag) relative to the maximum T_{air} due to *a)* the residence times of the flow path and *b)* the heat transfer and melt dynamics in the RG. We observe a clear trend in the lag between the S1 EC and T_{air} diurnal cycles during the snow-free period (Figure 8). The shift from $\sim$0 hours in July to ~ -5 hours in November implies a lag between maximum T_{air} and minimum EC of $\sim$12 hours during the warmest period and $\sim$7 hours during the coldest snow-free period. Although S4 appears more influenced by water from other sources, it exhibits a similar trend.

There are likely several factors that cause this seasonal trend in lag time between diurnal T_{air} maxima and EC minima. Firstly, the ice thickness in the active layer decreases throughout the snow-free period, implying increasingly shorter flowpaths throughout the melt season. Furthermore, preferential flow paths, akin to glaciar moulins, may also be formed internally by melt water throughout this period, further reducing the residence time. Secondly, as temperatures decrease, there will be proportionally less melt from higher-elevation zones of the rock glacier and thus the mean flow path length to the foot of the RG will decrease. Finally, during the warmest months, melt is expected to be continuous, while in the late season daily minimum temperatures are often <0°C. We posit that these processes combine to contribute to a delay between maximum air temperature and minimum spring EC that decreases throughout the snow-free period.

5.4 Intermittent flow and dilution intensities in springs

In the southern European Alps, the summer and autumn of 2022 were drier than average and followed a winter with exceptionally low snow accumulation (Choler, 2023). Because of this, the contribution of deeper groundwater to the springs (Figure 10) may have played a more important role than in average years. As discharged baseflow becomes more mineralised, the amplitude of dilution due to the diurnal freeze/thaw cycle of the RG ice may increase. At the end of winter, S1 reactivates as the snowpack melts, resulting in a large diurnal amplitude that is also visible in the spring discharge at the talus/meadow interface. This emphasises the importance of both snow- and ice-melt cycles as the cause of important oscillations in water parameters (Krainer and Mostler, 2002; Berger et al., 2004; Krainer et al., 2007) and the fact that these cycles smooth out during the summer (Brighenti et al., 2021). Based on these results, groundwater from the shallow fractured aquifer is the main component of the Canfinal RG discharge. Its discharge is strongly influenced in spring and until summer by snowmelt, which reactivates S1 with a daily dilution of greater amplitude and occurring earlier in the afternoon. Intermittent drying of springs S1–S3 was

https://doi.org/10.5194/egusphere-2024-927
Preprint. Discussion started: 14 May 2024

observed multiple times (Figure 7), with springs S2 and S3 (in the talus slope) only flowing continuously at the beginning of the snow-free period. These observations and the groundwater monitoring data (Figure 9B) indicate that groundwater levels are only high enough to sustain flow immediately after snowmelt. Flow in springs S2 and S3 later in the year is short-lived and caused by precipitation events. In contrast, spring S1, as discussed, is directly influenced by RG thawing which contributes to a groundwater table that remains at or near the surface throughout this period. Spring S4 is at the talus-meadow interface where the topographic gradient lessens and, as such, appears to have perennial flow assured by groundwater even when the water table is at its annual minimum. This water has a longer residence time as indicated by its higher mineralisation compared to the other three springs. During winter baseflow conditions, snow cover and large amounts of frozen ground prevent recharge of the fractured aquifer. As a result, the water table drops significantly and all springs are dry except for S4.

5.5 Refining the conceptual model for RG-groundwater interactions

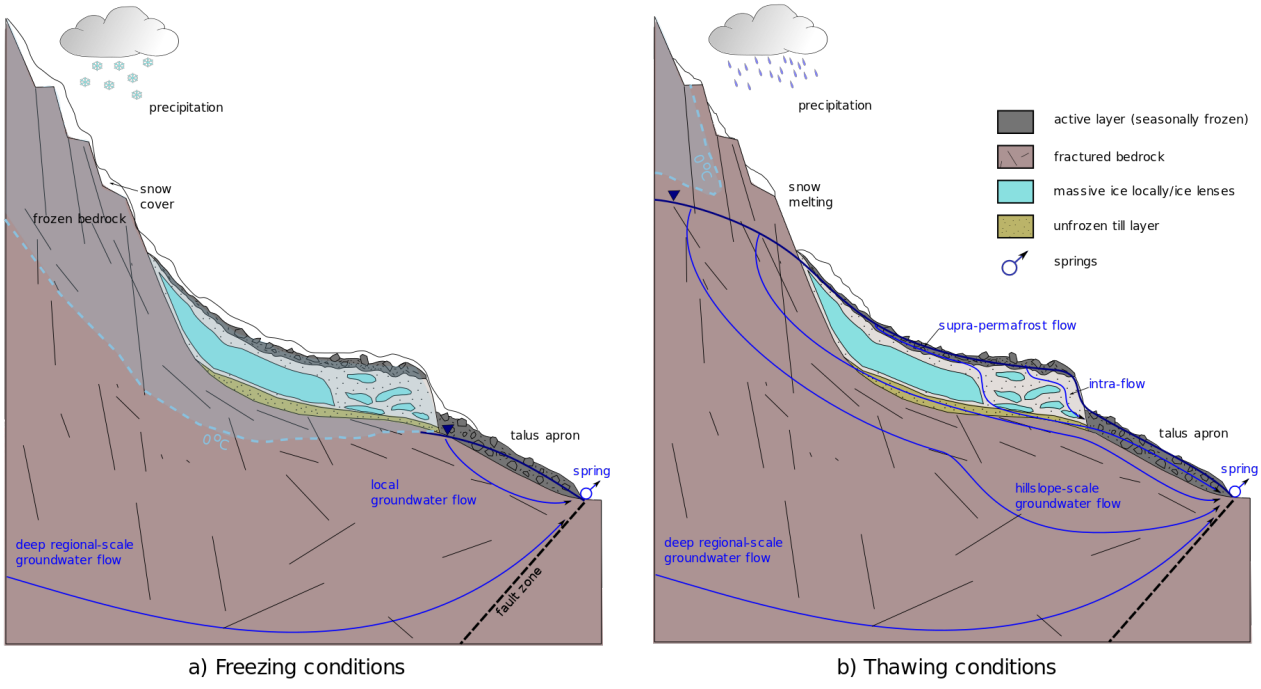

Figure 10. Conceptual model of the interaction between permafrost and mobile groundwater at the Canfinal RG during a) freezing conditions in winter and b) thawing conditions in summer. Modified from Jones et al. (2019).

The ensemble of our analyses allows us to propose a refined conceptual model for the hydrological and hydrogeological functioning of this system, taking into account the influence of the RG (Figure 10). Freeze/thaw cycles influence spring runoff and solute transport on seasonal and daily time scales. During winter, the shallow subsurface remains dominantly frozen, preventing groundwater recharge and confining groundwater flow to deep flow paths with longer residence times and higher solute

https://doi.org/10.5194/egusphere-2024-927
Preprint. Discussion started: 14 May 2024

concentrations. As temperatures rise during the summer, the active layer of permafrost thaws, re-enabling shallow groundwater flow paths. Meltwater from ice-rich RGs and permafrost discharges to down-gradient aquifers, springs and streams. Spring discharge rates and their composition in specific environmental tracers such as EC, ions and water stable isotopes vary as a result of freeze-thaw cycles. Melting of low EC ice from the RG results in dilution of down-gradient springs with effective residence times progressively decreasing until the return of freezing conditions.

6 Conclusions

Although RGs generally contain smaller quantities of water than glaciers (Wagner et al., 2021), their hydrological role is significant in many alpine catchments. Their rheological and hydrological state serves as an important climate change "barometer" for alpine environments where they are present. As climate change is expected to continue to impact the hydrological and hydrogeological dynamics of mountain headwater catchments (Evans et al., 2018; Somers et al., 2019; Arnoux et al., 2021; Halloran et al., 2023), hydrological understanding and monitoring of permafrost-groundwater interactions, including RG-spring connectivity, is paramount. We confirmed that the Canfinal RG is still active and that its creep rate appears to have accelerated in recent years alongside increasing temperature. Without measurements of the internal structure of the RG, it is not possible to reliably estimate the remaining "lifespan" of this active RG, although with increasing temperatures and decreasing snow cover, it is likely that it, like many RGs in the European Alps, will eventually become inactive. Geochemical and isotopic analyses enabled the differentiation of water sources contributing to the springs. The frequency-domain analyses in which we isolate the non-stationary 1 cpd components of EC and temperature provided valuable insights into the connectivity of the RG and springs, as well as their residence times. We have determined that the delay between diurnal air temperature maxima and dilution minima decreases over the snow-free period, implying a progressive decrease in RG-spring residence times, and have proposed several mechanisms for this phenomenon. We recommend that this type of approach be applied to additional sites to tests its limits in determining the temporal dynamics of permafrost-groundwater interactions. Monitoring of the RG interior via direct measurements or geophysical techniques, as well as numerical modelling, may provide us with a refined understanding of the internal hydrological processes in the Canfinal RG and other RGs. Our combination of remote sensing imagery, geochemical measurements, and hydrological monitoring has enabled a more comprehensive understanding of this fragile alpine hydrological system.

Author contributions. All authors wrote the manuscript collaboratively. CL: field work, laboratory analyses, data validation and analyses, figure creation, programming, and synthesis. LJSH & CR: supervision, field work, data analysis, programming, figure creation, synthesis, and project management.

Competing interests. The authors declare no competing interests.

https://doi.org/10.5194/egusphere-2024-927
Preprint. Discussion started: 14 May 2024

Acknowledgements. The authors would like to thank Luc Illien (GFZ Potsdam), Emilio Kenda, Noam Makkinga et Eliot Barbier (Université de Neuchâtel) for their assistance in the field. We also thank John Molson (Université de Laval) for interesting discussions about cryosphere processes. LJSH acknowledges funding from the Swiss National Science Foundation (SNSF Grant #212622, "RADMOGG").

https://doi.org/10.5194/egusphere-2024-927
Preprint. Discussion started: 14 May 2024

References

Acworth, R. I., Rau, G. C., Halloran, L. J. S., and Timms, W. A.: Vertical groundwater storage properties and changes in confinement determined using hydraulic head response to atmospheric tides, Water Resources Research, 53, 2983–2997, https://doi.org/10.1002/2016WR020311, ISBN: 6176273099, 2017.

Amschwand, D., Ivy-Ochs, S., Frehner, M., Steinemann, O., Christl, M., and Vockenhuber, C.: Deciphering the evolution of the Bleis Marscha rock glacier (Val d'Err, eastern Switzerland) with cosmogenic nuclide exposure dating, aerial image correlation, and finite element modeling, The Cryosphere, 15, 2057–2081, https://doi.org/10.5194/tc-15-2057-2021, publisher: Copernicus GmbH, 2021.

Amschwand, D., Scherler, M., Hoelzle, M., Krummenacher, B., Haberkorn, A., Kienholz, C., and Gubler, H.: Surface heat fluxes at coarse-blocky Murtèl rock glacier (Engadine, eastern Swiss Alps), EGUsphere (preprint), 2023, 1–56, https://doi.org/10.5194/egusphere-2023-2109, 2023.

Anderson, R. S., Anderson, L. S., Armstrong, W. H., Rossi, M. W., and Crump, S. E.: Glaciation of alpine valleys: The glacier – debris-covered glacier – rock glacier continuum, Geomorphology, 311, 127–142, https://doi.org/10.1016/j.geomorph.2018.03.015, 2018.

Arnoux, M., Brunner, P., Schaefli, B., Mott, R., Cochand, F., and Hunkeler, D.: Low-flow behavior of alpine catchments with varying quaternary cover under current and future climatic conditions, Journal of Hydrology, 592, 125 591, https://doi.org/10.1016/j.jhydrol.2020.125591, publisher: Elsevier, 2021.

Baltsavias, E. P.: Multiphoto geometrically constrained matching, Doctoral Thesis, Swiss Federal Institute of Technology, Zurich, https://doi.org/10.3929/ethz-a-000617558, 1991.

Berger, J., Krainer, K., and Mostler, W.: Dynamics of an active rock glacier (Ötztal Alps, Austria), Quaternary Research, 62, 233–242, https://doi.org/10.1016/j.yqres.2004.07.002, 2004.

Beria, H., Larsen, J. R., Ceperley, N. C., Michelon, A., Vennemann, T., and Schaefli, B.: Understanding snow hydrological processes through the lens of stable water isotopes, WIREs Water, 5, e1311, https://doi.org/10.1002/wat2.1311, 2018.

Bickel, V. T., Manconi, A., and Amann, F.: Quantitative Assessment of Digital Image Correlation Methods to Detect and Monitor Surface Displacements of Large Slope Instabilities, Remote Sensing, 10, 865, https://doi.org/10.3390/rs10060865, 2018.

Brighenti, S., Engel, M., Tolotti, M., Bruno, M. C., Wharton, G., Comiti, F., Tirler, W., Cerasino, L., and Bertoldi, W.: Contrasting physical and chemical conditions of two rock glacier springs, Hydrological Processes, 35, e14 159, https://doi.org/10.1002/hyp.14159, 2021.

Buchli, T., Kos, A., Limpach, P., Merz, K., Zhou, X., and Springman, S. M.: Kinematic investigations on the Furggwanghorn Rock Glacier, Switzerland, Permafrost and Periglacial Processes, 29, 3–20, https://doi.org/10.1002/ppp.1968, 2018.

Burga, C. A.: Gletscher- und Vegetationsgeschichte der Südrätischen Alpen seit der Späteiszeit, vol. 101 of *Denkschriften der Schweizerischen Naturforschenden Gesellschaft*, Birkhäuser, Basel - Boston, ISBN 978-3-0348-9986-4 978-3-0348-9301-5, http://link.springer.com/10.1007/978-3-0348-9301-5, 1987.

Cano-Paoli, K., Chiogna, G., and Bellin, A.: Convenient use of electrical conductivity measurements to investigate hydrological processes in Alpine headwaters, Science of The Total Environment, 685, 37–49, https://doi.org/10.1016/j.scitotenv.2019.05.166, 2019.

Choler, P.: Above-treeline ecosystems facing drought: lessons from the 2022 European summer heat wave, Biogeosciences, 20, 4259–4272, https://doi.org/10.5194/bg-20-4259-2023, 2023.

Cicoira, A., Marcer, M., Gärtner-Roer, I., Bodin, X., Arenson, L. U., and Vieli, A.: A general theory of rock glacier creep based on in-situ and remote sensing observations, Permafrost and Periglacial Processes, 32, 139–153, https://doi.org/10.1002/ppp.2090, 2021.

https://doi.org/10.5194/egusphere-2024-927
Preprint. Discussion started: 14 May 2024

Colombo, N., Salerno, F., Gruber, S., Freppaz, M., Williams, M., Fratianni, S., and Giardino, M.: Review: Impacts of permafrost degradation on inorganic chemistry of surface fresh water, Global and Planetary Change, 162, 69–83, https://doi.org/10.1016/j.gloplacha.2017.11.017, 2018.

Colombo, N., Salerno, F., Martin, M., Malandrino, M., Giardino, M., Serra, E., Godone, D., Said-Pullicino, D., Fratianni, S., Paro, L., Tartari, G., and Freppaz, M.: Influence of permafrost, rock and ice glaciers on chemistry of high-elevation ponds (NW Italian Alps), Science of The Total Environment, 685, 886–901, https://doi.org/10.1016/j.scitotenv.2019.06.233, 2019.

Cusicanqui, D., Rabatel, A., Vincent, C., Bodin, X., Thibert, E., and Francou, B.: Interpretation of Volume and Flux Changes of the Laurichard Rock Glacier Between 1952 and 2019, French Alps, Journal of Geophysical Research: Earth Surface, 126, e2021JF006 161, https://doi.org/10.1029/2021JF006161, 2021.

DallAmico, M., Endrizzi, S., Rigon, R., and Gruber, S.: The importance of snow cover evolution in rock glacier temperature modeling, 9th International Conference on Permafrost, Fairbanks, Alaska, pp. 57–58, 2008.

Del Siro, C., Scapozza, C., Perga, M.-E., and Lambiel, C.: Investigating the origin of solutes in rock glacier springs in the Swiss Alps: A conceptual model, Frontiers in Earth Science, 11, 1056 305, https://doi.org/10.3389/feart.2023.1056305, 2023.

Delaloye, R., Lambiel, C., and Gärtner-Roer, I.: Overview of rock glacier kinematics research in the Swiss Alps, Geographica Helvetica, 65, 135–145, https://doi.org/10.5194/gh-65-135-2010, 2010.

Duval, P., Ashby, M. F., and Anderman, I.: Rate-controlling processes in the creep of polycrystalline ice, The Journal of Physical Chemistry, 87, 4066–4074, https://doi.org/10.1021/j100244a014, 1983.

Evans, S. G., Ge, S., Voss, C. I., and Molotch, N. P.: The Role of Frozen Soil in Groundwater Discharge Predictions for Warming Alpine Watersheds, Water Resources Research, 54, 1599–1615, https://doi.org/10.1002/2017WR022098, 2018.

FOEN Switzerland: Map of potential permafrost distribution, https://www.geocat.ch/geonetwork/srv/eng/catalog.search#/metadata/71d087ef-6531-4131-98ea-88ff655d8a63, 2005.

Frei, P., Kotlarski, S., Liniger, M. A., and Schär, C.: Future snowfall in the Alps: projections based on the EURO-CORDEX regional climate models, The Cryosphere, 12, 1–24, https://doi.org/10.5194/tc-12-1-2018, 2018.

Groh, T. and Blöthe, J. H.: Rock Glacier Kinematics in the Kaunertal, Ötztal Alps, Austria, Geosciences, 9, 373, https://doi.org/10.3390/geosciences9090373, 2019.

Haeberli, W., Hallet, B., Arenson, L., Elconin, R., Humlum, O., Kääb, A., Kaufmann, V., Ladanyi, B., Matsuoka, N., Springman, S., and Mühll, D. V.: Permafrost creep and rock glacier dynamics, Permafrost and Periglacial Processes, 17, 189–214, https://doi.org/10.1002/ppp.561, _eprint: https://onlinelibrary.wiley.com/doi/pdf/10.1002/ppp.561, 2006.

Halloran, L. J., Millwater, J., Hunkeler, D., and Arnoux, M.: Climate change impacts on groundwater discharge-dependent streamflow in an alpine headwater catchment, Science of The Total Environment, 902, 166 009, https://doi.org/10.1016/j.scitotenv.2023.166009, 2023.

Hanus, S., Hrachowitz, M., Zekollari, H., Schoups, G., Vizcaino, M., and Kaitna, R.: Timing and magnitude of future annual runoff extremes incontrasting Alpine catchments in Austria, 2021.

Harrington, J. S., Mozil, A., Hayashi, M., and Bentley, L. R.: Groundwater flow and storage processes in an inactive rock glacier, Hydrological Processes, 32, 3070–3088, https://doi.org/10.1002/hyp.13248, 2018.

Harris, C., Arenson, L. U., Christiansen, H. H., Etzelmüller, B., Frauenfelder, R., Gruber, S., Haeberli, W., Hauck, C., Hölzle, M., Humlum, O., Isaksen, K., Kääb, A., Kern-Lütschg, M. A., Lehning, M., Matsuoka, N., Murton, J. B., Nötzli, J., Phillips, M., Ross, N., Seppälä, M., Springman, S. M., and Vonder Mühll, D.: Permafrost and climate in Europe: Monitoring and modelling thermal, geomorphological and geotechnical responses, Earth-Science Reviews, 92, 117–171, https://doi.org/10.1016/j.earscirev.2008.12.002, 2009.

https://doi.org/10.5194/egusphere-2024-927
Preprint. Discussion started: 14 May 2024

Hayashi, M.: Alpine Hydrogeology: The Critical Role of Groundwater in Sourcing the Headwaters of the World, Groundwater, 58, 498–510, https://doi.org/10.1111/gwat.12965, 2020.

Hersbach, H., Bell, B., Berrisford, P., Biavati, G., Horányi, A., Muñoz Sabater, J., Nicolas, J., Peubey, C., Radu, R., Rozum, I., Schepers, D., Simmons, A., Soci, C., Dee, D., and Thépaut, J.-N.: ERA5 hourly data on single levels from 1940 to present, https://doi.org/10.24381/cds.adbb2d47, 2023.

Houben, T., Pujades, E., Kalbacher, T., Dietrich, P., and Attinger, S.: From Dynamic Groundwater Level Measurements to Regional Aquifer Parameters— Assessing the Power of Spectral Analysis, Water Resources Research, 58, e2021WR031 289, https://doi.org/10.1029/2021WR031289, _eprint: https://onlinelibrary.wiley.com/doi/pdf/10.1029/2021WR031289, 2022.

Humlum, O.: Active layer thermal regime at three rock glaciers in Greenland, Permafrost and Periglacial Processes, 8, 383–408, https://doi.org/10.1002/(SICI)1099-1530(199710/12)8:4<383::AID-PPP265>3.0.CO;2-V, 1997.

Ikeda, A., Matsuoka, N., and Kääb, A.: Fast deformation of perennially frozen debris in a warm rock glacier in the Swiss Alps: An effect of liquid water, Journal of Geophysical Research: Earth Surface, 113, https://doi.org/10.1029/2007JF000859, 2008.

Jones, D. B., Harrison, S., Anderson, K., and Whalley, W. B.: Rock glaciers and mountain hydrology: A review, Earth-Science Reviews, 193, 66–90, https://doi.org/10.1016/j.earscirev.2019.04.001, 2019.

Jones, D. B., Harrison, S., Anderson, K., and Betts, R. A.: Author Correction: Mountain rock glaciers contain globally significant water stores, Scientific Reports, 11, 2021.

Kassambara, A. and Mundt, F.: Factoextra: Extract and Visualize the Results of Multivariate Data Analyses, r Package, Version 1.0.7, https://CRAN.R-project.org/package=factoextra, 2020.

Krainer, K. and He, X.: Flow velocities of active rock glaciers in the austrian alps, Geografiska Annaler: Series A, Physical Geography, 88, 267–280, 2006.

Krainer, K. and Mostler, W.: Hydrology of Active Rock Glaciers: Examples from the Austrian Alps, Arctic, Antarctic, and Alpine Research, 34, 142–149, https://doi.org/10.1080/15230430.2002.12003478, 2002.

Krainer, K., Mostler, W., and Spötl, C.: Discharge from active rock glaciers, Austrian Alps: A stable isotope approach, Austrian Journal of Earth Sciences, 100, 102–112, 2007.

Krainer, K., Bressan, D., Dietre, B., Haas, J. N., Hajdas, I., Lang, K., Mair, V., Nickus, U., Reidl, D., Thies, H., and Tonidandel, D.: A 10,300-year-old permafrost core from the active rock glacier Lazaun, southern Otztal Alps (South Tyrol, northern Italy), Quaternary Research, 83, 324–335, https://doi.org/10.1016/j.yqres.2014.12.005, 2015.

Kääb, A., Frauenfelder, R., and Roer, I.: On the response of rockglacier creep to surface temperature increase, Global and Planetary Change, 56, 172–187, https://doi.org/10.1016/j.gloplacha.2006.07.005, 2007.

Laudon, H. and Slaymaker, O.: Hydrograph separation using stable isotopes, silica and electrical conductivity: an alpine example, Journal of Hydrology, 201, 82–101, https://doi.org/10.1016/S0022-1694(97)00030-9, 1997.

Lindsay, E. R. P.: Reversible recharge-related groundwater fluctuation and ground surface deformation at Alp Canfinal, Switzerland, Master's thesis, Swiss Federal Institute of Technology Zurich, Department of Earth Sciences, Zurich, 2000.

Longinelli, A. and Selmo, E.: Isotopic composition of precipitation in Italy: a first overall map, Journal of Hydrology, 270, 75–88, https://doi.org/10.1016/S0022-1694(02)00281-0, 2003.

Longinelli, A., Anglesio, E., Flora, O., Iacumin, P., and Selmo, E.: Isotopic composition of precipitation in Northern Italy: Reverse effect of anomalous climatic events, Journal of Hydrology, 329, 471–476, https://doi.org/10.1016/j.jhydrol.2006.03.002, 2006.

https://doi.org/10.5194/egusphere-2024-927
Preprint. Discussion started: 14 May 2024

Lê, S., Josse, J., and Husson, F.: FactoMineR: An R Package for Multivariate Analysis, Journal of Statistical Software, 25, 1–18, https://doi.org/10.18637/jss.v025.i01, 2008.

Manchado, A. M.-T., Allen, S., Cicoira, A., Wiesmann, S., Haller, R., and Stoffel, M.: 100 years of monitoring in the Swiss National Park reveals overall decreasing rock glacier velocities, Communications Earth & Environment, 5, 1–17, https://doi.org/10.1038/s43247-024-01302-0, publisher: Nature Publishing Group, 2024.

Marcer, M., Cicoira, A., Cusicanqui, D., Bodin, X., Echelard, T., Obregon, R., and Schoeneich, P.: Rock glaciers throughout the French Alps accelerated and destabilised since 1990 as air temperatures increased, Communications Earth & Environment, 2, 1–11, https://doi.org/10.1038/s43247-021-00150-6, 2021.

Moran, T. A., Marshall, S. J., Evans, E. C., and Sinclair, K. E.: Altitudinal Gradients of Stable Isotopes in Lee-Slope Precipitation in the Canadian Rocky Mountains, Arctic, Antarctic, and Alpine Research, 39, 455–467, https://doi.org/10.1657/1523-0430(06-022)[MORAN]2.0.CO;2, 2007.

Munroe, J. S. and Handwerger, A. L.: Contribution of rock glacier discharge to late summer and fall streamflow in the Uinta Mountains, Utah, USA, Hydrology and Earth System Sciences, 27, 543–557, https://doi.org/10.5194/hess-27-543-2023, 2023.

Pedregosa, F., Varoquaux, G., Gramfort, A., Michel, V., Thirion, B., Grisel, O., Blondel, M., Prettenhofer, P., Weiss, R., Dubourg, V., Vanderplas, J., Passos, A., Cournapeau, D., Brucher, M., Perrot, M., and Duchesnay, E.: Scikit-learn: Machine Learning in Python, Journal of Machine Learning Research, 12, 2825–2830, http://jmlr.org/papers/v12/pedregosa11a.html, 2011.

Pruessner, L., Phillips, M., Farinotti, D., Hoelzle, M., and Lehning, M.: Near-surface ventilation as a key for modeling the thermal regime of coarse blocky rock glaciers, Permafrost and Periglacial Processes, 29, 152–163, https://doi.org/10.1002/ppp.1978, 2018.

Pruessner, L., Huss, M., Phillips, M., and Farinotti, D.: A Framework for Modeling Rock Glaciers and Permafrost at the Basin-Scale in High Alpine Catchments, Journal of Advances in Modeling Earth Systems, 13, e2020MS002 361, https://doi.org/10.1029/2020MS002361, 2021.

Rau, G. C., Halloran, L. J. S., Cuthbert, M. O., Andersen, M. S., Acworth, R. I., and Tellam, J. H.: Characterising the dynamics of surface water-groundwater interactions in intermittent and ephemeral streams using streambed thermal signatures, Advances in Water Resources, 107, 354–369, https://doi.org/10.1016/j.advwatres.2017.07.005, 2017.

Schaffer, N., MacDonell, S., Réveillet, M., Yáñez, E., and Valois, R.: Rock glaciers as a water resource in a changing climate in the semiarid Chilean Andes, Regional Environmental Change, 19, 1263–1279, https://doi.org/10.1007/s10113-018-01459-3, 2019.

Somers, L. D. and McKenzie, J. M.: A review of groundwater in high mountain environments, WIREs Water, 7, e1475, https://doi.org/10.1002/wat2.1475, 2020.

Somers, L. D., McKenzie, J. M., Mark, B. G., Lagos, P., Ng, G. C., Wickert, A. D., Yarleque, C., Baraër, M., and Silva, Y.: Groundwater Buffers Decreasing Glacier Melt in an Andean Watershed—But Not Forever, Geophysical Research Letters, 46, 13 016–13 026, https://doi.org/10.1029/2019GL084730, 2019.

Wagner, T., Kainz, S., Krainer, K., and Winkler, G.: Storage-discharge characteristics of an active rock glacier catchment in the Innere Ölgrube, Austrian Alps, Hydrological Processes, 35, e14 210, https://doi.org/10.1002/hyp.14210, 2021.

Wei, T. and Simko, V.: R package 'corrplot': Visualization of a Correlation Matrix, https://github.com/taiyun/corrplot, version 0.92, https://github.com/taiyun/corrplot, 2021.

Williams, M. W., Knauf, M., Caine, N., Liu, F., and Verplanck, P. L.: Geochemistry and source waters of rock glacier outflow, Colorado Front Range, Permafrost and Periglacial Processes, 17, 13–33, https://doi.org/10.1002/ppp.535, 2006.

https://doi.org/10.5194/egusphere-2024-927
Preprint. Discussion started: 14 May 2024

Williams, M. W., Knauf, M., Cory, R., Caine, N., and Liu, F.: Nitrate content and potential microbial signature of rock glacier outflow, Colorado Front Range, Earth Surface Processes and Landforms, 32, 1032–1047, https://doi.org/10.1002/esp.1455, 2007.

Wirz, V., Gruber, S., Purves, R. S., Beutel, J., Gärtner-Roer, I., Gubler, S., and Vieli, A.: Short-term velocity variations at three rock glaciers and their relationship with meteorological conditions, Earth Surface Dynamics, 4, 103–123, https://doi.org/10.5194/esurf-4-103-2016, 2016.

Zhang, T.: Influence of the seasonal snow cover on the ground thermal regime: An overview, Reviews of Geophysics, 43, RG4002, https://doi.org/10.1029/2004RG000157, 2005.